

0038-1098(94)00915-5

RESISTIVITY SATURATION IN ALKALI-DOPED C₆₀

J. G. Hou[*], Li Lu, Vincent H. Crespi, X.-D. Xiang, A. Zettl and Marvin L. Cohen

Department of Physics
University of California at Berkeley
Berkeley, California 94720and
Materials Sciences Division, Lawrence Berkeley Laboratory
Berkeley, California 94720*(Received 27 October 1994; accepted in revised form 8 December 1994 by S. G. Louie)*

The high-temperature resistivity of K and Rb-doped C₆₀ single crystals was measured with pulsed heating techniques and analyzed within the parallel-resistor extension to Bloch-Boltzmann transport theory. Rb₃C₆₀ exhibits resistivity saturation with $\rho_{sat}^{Rb} \approx 6 \pm 3 \text{ m}\Omega\text{-cm}$, corresponding to a saturation mean free path of $\ell_{sat}^{Rb} \approx 1 \pm 0.5 \text{ \AA}$. In contrast K₃C₆₀ does not show signs of resistivity saturation up to 800 K, suggesting that $\rho_{sat}^K > 3 \text{ m}\Omega\text{-cm}$ and $\ell_{sat}^K < 1.5 \text{ \AA}$. The electronic states at high temperature have a characteristic length scale significantly smaller than the fcc lattice constant.

Keywords: fullerenes, electron-phonon interactions, electronic transport

The family of alkali-doped fullerenes contains the highest- T_c isotropic three dimensional superconductors presently known. Several experimental results point towards electron-phonon mediated superconductivity in these materials. In particular, the carbon isotope effect is substantial[1, 2] and both Raman measurements[3] and inelastic neutron scattering[4] yield phonon linewidths consistent with moderately strong electron-phonon coupling. Theoretical calculations of the electron-phonon coupling lend additional credence to this model[5, 6, 7, 8]. On the other hand, the alkali-doped fullerenes have several characteristics which suggest that the detailed preconditions of the standard BCS theory may not be fulfilled. The characteristic phonon energy scale ($\approx 0.1 \text{ eV}$) approaches the energy scale of intraband electronic dynamics ($\approx 0.4 \text{ eV}$). Calculations of metallic screening in the doped material suggest that the Coulomb interaction is efficiently screened, but with the possibility of a significant long-range Hubbard U[9]. Measurements of normal-state transport properties provide a means to evaluate the degree to which these materials can be described within Bloch-Boltzmann transport theory, a treatment

which assumes a separation of vibrational and electronic timescales and a single-particle view of electron dynamics. In particular, Bloch-Boltzmann theory predicts its own demise: a “run-of-the-mill” conductor will exhibit resistivity saturation as the mean free path approaches the interatomic spacing. The low temperature mean free path in the alkali-doped fullerenes is fairly short, suggesting that these materials are plausible candidates for the observation of resistivity saturation at high temperatures. However, if the alkali-doped fullerenes are dominated by correlative or nonadiabatic effects they will not necessarily be hostage to high-temperature resistivity saturation.

Previous experimental work has been interpreted as evidencing an absence of saturation for temperatures up to 550 K in K₃C₆₀ and Rb₃C₆₀ thin films[10]. These measurements were taken to support the possibility of novel transport mechanisms such as resonant tunnelling. However, as pointed out by these authors, an accurate evaluation of the high temperature resistivity in these materials requires a detailed consideration of the temperature dependent density of states, an effect which could mask the signature of resistivity saturation.

We report the first high temperature pulsed heating resistivity measurements up to 800 K on K- and Rb-doped C₆₀ single crystals. The data are analyzed within

[*] Present address: Dept. of Chemistry, Oregon State University, Corvallis, OR 97331-4003.

the parallel-resistor extension to Bloch-Boltzmann transport theory[12] with a temperature-dependent density of states to obtain a saturation mean free path of $l_{sat} \approx 1 \pm 0.4 \text{ \AA}$ for Rb_3C_{60} , on the order of the carbon-carbon bond length of 1.4 \AA . K_3C_{60} does not show obvious signs of saturation up to 800 K, suggesting an upper bound of $l_{sat} < 1.5 \text{ \AA}$. Both results are consistent with the expectations of resistivity saturation within Bloch-Boltzmann transport theory. These results indicate that the electronic states relevant to high-temperature transport have a characteristic length scale significantly smaller than the fcc lattice constant.

Single crystals of C_{60} were doped with Rb and K in the standard fashion[13], with iterative dope/anneal stages proceeding until a final resistivity minimum is reached. Since the metallic phase A_3C_{60} ($A = K, Rb$) is not the saturation phase of the intercalation process, it is useful to ask if a uniform A_3C_{60} phase can be easily obtained in a bulk sample. In this context we note that direct resistivity measurements on bulk samples yield results which are 2-3 \times higher than estimates based on various indirect, theoretical, or optical probes[14, 15, 16, 17, 18, 19]. Doping of bulk samples most likely begins with the formation of islands of doped material in pristine C_{60} . The finite vacancy energy of A_3C_{60} guarantees that the equilibrium dopant concentration at moderate temperature and dopant level will be somewhat substochiometric. In addition, at sufficiently high doping rate it may become possible to nucleate A_4C_{60} or A_6C_{60} inside the doped portions of the sample before the substochiometric A_3C_{60} phase diffuses through the crystal. A heterogeneous doping profile would account for the discrepancy between direct and indirect measurements of the DC resistivity in A_3C_{60} . We emphasize that the *functional form* of the temperature dependent resistivity is independent of detailed doping profile. Modulo differences in effective geometry, the temperature dependent resistivity of different samples of both K_3C_{60} and Rb_3C_{60} is precisely reproducible.

A major concern of high-temperature resistivity measurements in these materials is the possibility of thermally-driven rearrangement of the intercalant species, in particular deintercalation and/or formation of A_4C_{60} , A_6C_{60} , or solid solution A_xC_{60} phases at high temperature. To minimize these effects we use a pulsed heating apparatus which can heat the sample from room temperature to 800 K on a timescale of a few seconds. A tungsten heating element is bonded to a small ($2 \text{ mm} \times 2 \text{ mm}$) sapphire slab onto which the A_3C_{60} sample is attached with four $0.002''$ diameter gold wires in a stress-free configuration. The samples are typically $500 \times 150 \times 65 \text{ \mu m}$, small enough to ensure that the wires provide good thermal contact with the substrate. The sample temperature is measured with a miniature type-E thermocouple bonded directly to the top of the sample. The sample resistance is measured using a high-speed ac technique to avoid spurious thermal EMF's.

Fig. 1 shows the results of several runs of pulsed heating on single samples of both K_3C_{60} and Rb_3C_{60} . The dashed lines below 300 K are dc resistivity data for the

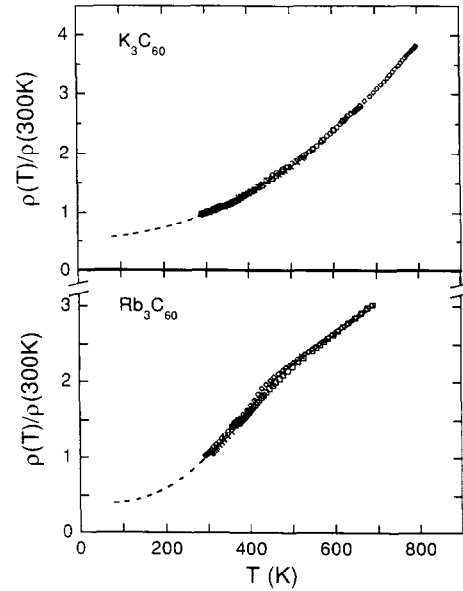


Figure 1: High temperature resistivity of K_3C_{60} and Rb_3C_{60} . Different symbols represent sequential pulsed heating runs. Data for $T < 300 \text{ K}$ (dashed lines) were obtained using conventional slow-cooling techniques.

same samples obtained by the more conventional slow-cooling technique. The high-temperature data in Fig. 1 are reproducible over several pulsed heating excursions, indicating minimal deintercalation or irreversible intercalant rearrangement. Similar results were obtained for different crystals of K_3C_{60} and Rb_3C_{60} . We note that freshly doped samples of K_3C_{60} often exhibit an interesting resistive anomaly near 380 K consisting of small, smooth hysteretic resistive step of order 10%, possibly accompanied by a very slight change in slope. This anomaly is also observed in samples that are heated in a non-pulsed manner. The origin of this anomaly is at present unclear, but it may reflect a change in effective geometry of the conducting portion of the sample or a change in lattice constant in the A_3C_{60} portion of the sample, either a stress-induced expansion due to a structural transition in a minority phase or an expansion local to the A_3C_{60} phase due to an orientational order/disorder transition in the doped material. In any case, this anomaly is "annealed out" and disappears after one or two high temperature cycles of the sample, yielding the smooth and reproducible $\rho(T)$ behavior shown in Fig. 1.

Turning to data analysis, we begin with a discussion of the theoretical treatment of resistivity saturation. Bloch-Boltzmann transport theory fails as the electronic mean free path approaches the lattice spacing. One can account for this effect by imposing a phenomenological minimum electron scattering time τ_{sat} , which corresponds to a length scale, $l_{sat} = \tau_{sat} v_f$, on the order of the interatomic spacing. This minimal time acts as an offset to the Poisson distribution of electron scattering events, yielding a parallel resistor model of resistivity saturation,[12, 11]

$$\frac{1}{\rho} = \frac{1}{\rho_{BB}} + \frac{1}{\rho_{sat}}. \quad (1)$$

At all temperatures, the finite offset τ_{sat} yields a resistivity slightly lower than that expected from conventional transport theory. At high temperatures, the resistivity eventually saturates at the value ρ_{sat} . The Bloch-Boltzmann resistivity ρ_{BB} is composed of two parts, a residual resistivity ρ_0 and an electron-phonon resistivity ρ_{ep} , which are assumed to contribute additively in accord with Matthiessen's rule. The electron-phonon contribution is modelled within the Ziman resistivity formula[20],

$$\rho(T) = \frac{8\pi^2}{\omega_p^2 k_B T} \int_0^{\omega_{max}} \frac{\hbar \omega \alpha_{tr}^2 F(\omega)}{\cosh\left(\frac{\hbar \omega}{k_B T}\right) - 1} d\omega, \quad (2)$$

where ω_p is the plasma frequency and $\alpha_{tr}^2 F(\omega)$ the frequency dependence of the transport-relevant electron-phonon coupling. We approximate $\alpha_{tr}^2 F(\omega)$ with the form of the coupling relevant to superconductivity, namely $\alpha^2 F(\omega)$. The transport form is weighed by the differences in Fermi velocities between the electronic states— for isotropic coupling the forms are identical. We take three different models of the on-ball contributions to $\alpha^2 F(\omega)$ with different weights of contributions from the range of on-ball phonon frequencies. These models yield average phonon frequencies of $\bar{\omega} \sim 500K$ [5], $\bar{\omega} \sim 1200K$ [6], $\bar{\omega} \sim 2000K$ [7]. Each model is augmented by the addition of variable coupling to a low-frequency mode set at $\omega = 150K$. This low frequency mode is a generic representation of possible contributions from alkali atom optic modes, librational modes, or interball translational modes. In all cases, the coupling to this mode turns out to be small, and the important features of the calculated resistivity are not sensitive to variations in the frequency of this mode from 50 to 200 K.

At first sight one might think that the presence of resistivity saturation could simply be read off of a graph of resistivity versus temperature. However, the special properties of the alkali-doped fullerenes necessitate a detailed theoretical treatment. In particular, the characteristic phonon frequency is quite high; within the experimentally accessible temperature range the system may never reach the high-T limit in which the resistivity is strictly proportional to the temperature. More importantly, the density of states at the Fermi level $N(0)$ for the alkali-doped fullerenes is a sensitive function of the lattice constant which varies considerably due to thermal expansion. Any application of standard results for interpreting the temperature dependence of a metallic resistivity (i.e. zero temperature back-extrapolation, high-temperature linearity) must proceed with caution in light of this strong temperature dependence. The electron-phonon component of the resistivity is expected to be proportional to the density of states squared, one factor of $N(0)$ from ω_p^2 , another from the scattering time in the formula $\rho_{ep} = \frac{4\pi}{\omega_p^2 \tau}$ where ω_p is the plasma frequency. Alternatively, the density of states dependence can be recast as a dependence on Fermi velocity wherein the conductivity is proportional to Fermi velocity squared.

Taking $v_f \sim \frac{1}{N(0)}$, we again obtain a resistivity proportional to density of states squared. An increasing $N(0)$ as a function of T will contribute positive curvature to $\rho(T)$, obscuring the signature of saturation. The temperature dependence of the residual resistivity is less clear. Theoretically, one expects a density of states dependence to the residual resistivity if the residual scattering mechanism is slaved to a microscopic time scale or energy scale, and a density of states-independent residual resistivity if the mechanism is slaved to a microscopic length scale, as suggested by Gelfand and Lu[18]. Experimentally, the residual resistivity of Rb₃C₆₀ shows a significant pressure dependence[21]. In addition, several sources of information[10, 14, 15, 16] indicate that the residual resistivity in K₃C₆₀ is roughly $\frac{1}{2}$ of the residual resistivity of Rb₃C₆₀, a difference which could be attributed to the difference in density of states between these two materials. In the present analysis we assume that the residual resistivity scales as the density of states squared. Should this assumption be in error, the effect upon the final results should be small since the low temperature residual resistivity is a small fraction of the total resistivity at high temperatures. Lastly, we note that although the low frequency interball phonons will be strongly temperature dependent, the fits to the Ziman formula suggest that the coupling to these modes is small.

We obtain the temperature dependent density of states by combining the density of states as a function of lattice constant from a LDA band-structure calculation[22] with the experimental coefficient of thermal expansion to yield the density of states as a function of temperature. Although the actual system is orientationally disordered, the disorder serves primarily to smear out the fine structure in the density of states[23]— the *scaling* of density of states with lattice constant should be similar to that of the ordered system. In fact, the result for the ordered system is in reasonably good agreement with NMR measurements of the temperature dependence of $\sqrt{\frac{1}{T_1 T}}$ [24]. The thermal expansion for both K₃C₆₀[25] and Rb₃C₆₀[26] has been measured from 5 K to 300 K. Above 100 K the lattice constant is accurately modelled with a linear temperature dependence, the form chosen for extrapolation to 800 K. The density of states has been calculated for lattice constants from 14.0 Å to 14.435 Å. Treatment of the Rb₃C₆₀ experiment requires extrapolation beyond the range of calculated values. We compared two functional forms for this extrapolation, a least squares cubic polynomial fit, and a fit to the form $N(a) = N_o (a - \bar{a})^\eta$, with $N_o = 0.058 \frac{1}{eV C_{60}}$, $\bar{a} = 10.21$ Å and $\eta = 4.34$ as fitting parameters. Both forms yield comparable fits with similar extrapolations. The variations in extrapolation are taken into account in the estimation of uncertainties.

We normalize the experimentally determined resistivity curves by appeal to an analysis of upper critical field data which yields values of the T=0 scattering time.[15, 16] Combining these results with theoretical values for the plasma frequencies of K₃C₆₀ and Rb₃C₆₀ (1.2 and 1.11 eV respectively)[27, 28] yields values of the T=0 resistivity of $0.18 \pm 0.06 m\Omega\text{-cm}$ and $0.57 \pm 0.21 m\Omega\text{-cm}$.

cm respectively, in reasonable accord with theoretical calculations[18, 17]. Normalizing the data of Fig. 1 to these values yields the absolute resistivity curves in Fig. 2 (open circles). The shaded areas indicate the range of uncertainty in the normalization. Representative theoretical fitting curves are included in this figure.

Two ancillary points are immediately evident from the theoretical analysis. First, a temperature-dependent density of states is necessary to obtain a satisfactory fit to the full range of experimental data for K_3C_{60} . The continuous (dashed) curve following the K_3C_{60} data in Fig. 2 shows the best fit with (without) a temperature-dependent density of states for the model with $\bar{\omega} \approx 1200K$. The fit at constant $N(0)$ is substantially worse. Secondly, the fits using the coupling spectrum with lowest average frequency ($\bar{\omega}=500$ K) are quite poor, as evidenced by the dashed fit to the Rb_3C_{60} data in Fig 2. This result suggests that the relative contributions of on-ball phonons to the electron-phonon coupling is centered at moderate to high frequencies. Finally, we note that the values of the total electron-phonon coupling λ derived from these analyses are in accord with the range expected for a BCS superconductor[29].

The high-temperature resistivity of Rb_3C_{60} is in reasonably good agreement with the parallel resistor model of saturation. The data deviates from the fitted form at the highest temperatures, perhaps suggestive of the limitations of the phenomenological parallel resistor model or

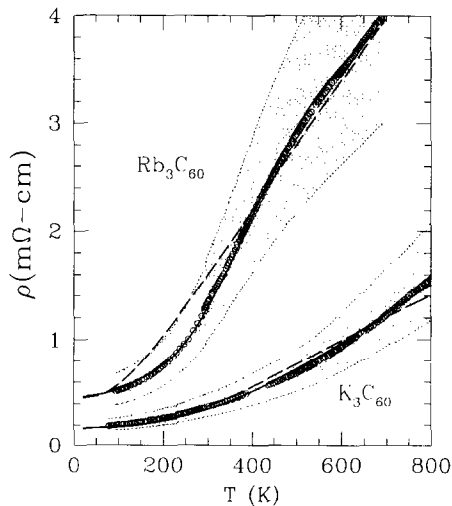


Figure 2: Normalized resistivity versus temperature for K_3C_{60} (lower curve) and Rb_3C_{60} (upper curve). Shaded areas indicate uncertainties in resistivity normalization. Solid and dashed curves are theoretical fits. For Rb_3C_{60} the dashed line fit uses the electron-phonon coupling spectrum from Jishi et al. ($\bar{\omega} \approx 500$ K), whereas the solid line fit uses the spectrum of Varma et al. ($\bar{\omega} \approx 2000K$). Both models include a temperature-dependent density of states. The fits to the K_3C_{60} data use the coupling spectrum from Schluter et al. ($\bar{\omega} \approx 1200$ K). The solid fit includes a temperature-dependent density of states whereas the dashed fit does not.

of the Bloch-Boltzman transport theory itself. The spectrum with $\bar{\omega} \approx 1200K$ yields $\rho_{sat} = 5.1 \pm 1.9 m\Omega\text{-cm}$ while the model with $\bar{\omega} \approx 2000K$ yields $\rho_{sat} = 6.3 \pm 2.4 m\Omega\text{-cm}$ (this fit is shown in Fig. 2 as the solid curve following the Rb_3C_{60} data). The saturation length can be derived from these values by appeal to theoretical values for the plasma frequency and Fermi velocity (1.8×10^7 cm/sec for K_3C_{60} and 1.6×10^7 cm/sec for Rb_3C_{60}) which are obtained from LDA electronic structure calculations in the orientationally ordered structure[27, 28]. The results for Rb_3C_{60} are $\ell_{sat} = 0.9 \pm 0.4 \text{ \AA}$ for $\bar{\omega} \approx 1200$ K and $\ell_{sat} = 1.0 \pm 0.5 \text{ \AA}$ for $\bar{\omega} \approx 2000$ K, saturation lengths on the order of the carbon-carbon bond length.

The K-doped sample does not show obvious signs of saturation. The theoretical analysis yields a lower bound on the magnitude of the saturation resistivity. The solid curve following the K_3C_{60} data in Fig. 2 is the best fit to the model with $\bar{\omega} \approx 1200$ K and $\rho_{sat} = 6.4 \pm 2.0 m\Omega\text{-cm}$. Smaller values of ρ_{sat} yield unsatisfactory fits to the data. The model with $\bar{\omega} \approx 2000$ K yields an analogous bound of $\rho_{sat} > 4.8 \pm 1.5 m\Omega\text{-cm}$. Taking $4.8 \pm 1.5 m\Omega\text{-cm}$ as a lower bound on ρ_{sat} yields a bound on the saturation length of $\ell_{sat} < 1.1 \pm 0.4 \text{ \AA}$. Like the situation for Rb_3C_{60} , this value is consistent with the C-C bond length. A comparison of the normalized resistivity data for K_3C_{60} and Rb_3C_{60} in Fig. 2 clearly shows that even at the highest temperatures reported (~ 800 K) the K_3C_{60} sample has not yet reached a resistivity regime similar to that in which the Rb_3C_{60} sample begins to exhibit resistivity saturation.

We note two experimental uncertainties which could have significant impact of the conclusions of this work. First, the absolute value of the resistivity is somewhat in question. We note that estimates of the resistivity from fluctuation measurements[14] are smaller than the values used in the present analysis. Using these fluctuation-derived values would yield saturation lengths $2\times$ larger for Rb_3C_{60} and $1.5\times$ larger for K_3C_{60} . On the other hand, if one believes that the direct measurements of the resistivity represent intrinsic properties, one obtains saturation lengths roughly $2\text{-}3\times$ shorter than derived in this work. These values, substantially smaller than the carbon-carbon bond length, would be at odds with the parallel resistor extension to Bloch-Boltzmann transport theory. We believe that the direct measurements of the absolute resistivity are least accurate due to uncertainties in the effective volume of the sample. Second, we note that an experimental measurement of the low-temperature *constant volume* resistivity[21] suggests that the spurious positive curvature introduced by constant pressure measurement is substantially greater than that predicted by a temperature dependent density of states, indicating that the signature of saturation adjusted to constant sample volume may be stronger than that resulting from the present analysis, yielding a longer ℓ_{sat} . Detailed consideration of this point awaits experimental data on the constant volume resistivity at higher temperatures. Finally, we remark that inclusion of the temperature dependence of the low frequency interball modes would yield slightly ($\sim 10\%$) longer saturation mean free

paths without substantively altering the conclusions of the analysis.

Measurements of the high-temperature resistivity in K₃C₆₀ and Rb₃C₆₀ imply that the electronic mean free path has a minimal value on the order of the carbon-carbon bond length. These results indicate that the single particle states relevant to transport at high temperature have a characteristic length scale much smaller than the fcc lattice constant of roughly 14 Å. Although calculations for the orientationally disordered A₃C₆₀ lattice [17] suggest that the extended-state description of electron dynamics is applicable at T=0, the present work indicates

that the character of the appropriate electronic states changes significantly from low to high temperatures.

Acknowledgements- We have benefited greatly from the experimental assistance of J. Hone and from discussions with A. F. Hebard, J. H. Weaver, W. A. Vareka, B. Burk, and S. C. Erwin. This work was supported by National Science Foundation Grants No. DMR-90-17254 (JH, XX, LL and AZ) and DMR-9120269 (VHC and MLC), and the Director, Office of Energy Research, Office of Basic Energy Sciences, Materials Sciences Division of the U. S. Department of energy under Contracts No. DE-AC03-76SF00098.

REFERENCES

1. C.-C. Chen and C. M. Lieber, *Jour. of the Amer. Chem. Soc.* **114**, 3141 (1992).
2. A. P. Ramirez et al., *Phys. Rev. Lett.* **68**, 1058 (1992).
3. M. G. Mitch, S. J. Chase and J. S. Lannin, *Phys. Rev. Lett.* **68**, 883 (1992).
4. K. Prassides et al., *Nature* **354**, 462 (1991).
5. R. A. Jishi and M. S. Dresselhaus, *Phys. Rev. B* **45**, 2597 (1992).
6. M. Schluter, M. Lannoo, M. Needles, and G. A. Baraff, *Phys. Rev. Lett.* **68**, 526 (1992).
7. C. M. Varma, J. Zaanen and K. Raghavachari, *Science* **245**, 989 (1991).
8. I. I. Mazin, O. V. Dolgov, A. Golubov and S. V. Shulga, *Phys. Rev. B* **47**, 538 (1993).
9. O. Gunnarsson and G. Zwirner, *Phys. Rev. Lett.* **69** 957 (1992).
10. A. F. Hebard, T. T. M. Palstra, R. C. Haddon and R. M. Fleming, *Phys. Rev. B* **48**, 9945 (1993).
11. M. Gurvitch, *Phys. Rev. B* **24**, 7407 (1981).
12. P. B. Allen in *Superconductivity in d- and f-Band Metals*, ed. H. Suhl and M. B. Maple (Academic Press, New York 1980) p. 291.
13. X.-D. Xiang et al., *Science* **256**, 1190 (1992).
14. X.-D. Xiang et al., *Nature* **361**, 54 (1993).
15. J. G. Hou et al., *Solid State Comm.* **86**, 643 (1993).
16. J. G. Hou et al., *Physica C* **228**, 175 (1994).
17. E. J. Mele and S. C. Erwin, unpublished.
18. J. P. Lu and M. Gelfand, *Phys. Rev. B* **46**, 4367 (1992).
19. L. D. Rotter et al., *Nature* **355**, 532 (1992).
20. G. Grimvall, *The electron-phonon interaction in metals*, North-Holland Publishing Company, (1991) p.p 210-223.
21. W. A. Vareka, and A. Zettl, *Phys. Rev. Lett.* **72**, 4121 (1994).
22. A. Oshiyama and S. Saito, *Solid State Comm.* **82**, 41 (1992).
23. J. P. Lu and M. Gelfand, *Phys. Rev. Lett.* **68**, 1050 (1992).
24. R. Tycko et al., *Phys. Rev. Lett* **68**, 1912 (1992).
25. K. Prassides, personal communication.
26. P. W. Stephens et al., *Phys. Rev. B* **45**, 543 (1992).
27. S. C. Erwin and W. E. Pickett, *Science* **254**, 842 (1991).
28. S. C. Erwin, personal communication of Fermi velocity and plasma frequency of K₃C₆₀ at the Rb₃C₆₀ lattice constant.
29. V. H. Crespi et al., *Phys. Rev B* **46**, 12064 (1992).